ON AN EXPERIMENTALLY VALIDATED METHODOLOGY FOR PREDICTING THE BEARING STRENGTH OF FIBRE METAL LAMINATES

Peter P. Krimbalis*, Cheung J. Poon*, Kamran Behdinan*, Zouheir Fawaz*
[Peter P. Krimbalis]: p2krimba@ryerson.ca
***Ryerson University, 350 Victoria Street, Toronto, Ontario, Canada, M5B 2K3**

Keywords: *fibre metal laminates, GLARE, bearing strength, characteristic length method, delamination buckling, finite element method, experimental methodology*

Abstract

A novel methodology for predicting the bearing strength of fibre metal laminates (FMLs) was developed and implemented based on theoretical and empirical results. Finite element (FE) analyses were carried out on layer by layer models of several variants of GLARE and lead to a redefinition of the compressive characteristic dimension (CCD). The new definition is governed by the yield strength of aluminum and it was shown, analytically, that the contribution of the glass layers to bearing strength, in a bearing mode, is negligible. As a result, it was proposed that bearing strength in FMLs is governed by delamination and yielding of the aluminum layers. A novel experimental methodology was then designed using strain gauges to measure the local deformation of a pin bearing configuration based on the new CCD definition. Novel bearing strength versus measured strain curves were generated which lead to a redefinition of bearing yield and a complete characterization of the material response. Yielding has in fact occurred within the predicted CCD distance - according to the new definition(s) - and further work is currently underway to support this notion further.

1 Introduction

The recent development of GLAss REinforced (GLARE) FMLs represents the newest application of hybrid composites to aerospace structures. Developed in the Netherlands, FMLs are a consolidation of alternating layers of either 7075 or 2024-T3 aluminum alloy, coupled with unidirectional S_2-glass fibres embedded in an epoxy matrix [1]. The result is a laminated structure exhibiting superior properties when compared to monolithic aluminum and one whose application can be tailored via adjustments to fibre orientation and volume of aluminum.

A number of investigations into the pin and bolt bearing behaviour of FMLs can be found in the literature [2-5] however, the focus of these methodologies has not been on a concentrated examination of the associated strain field near the fastener hole. Instead, the principal aim has been the generation of bearing strength values, which although useful, provide little intuition regarding the failure mechanism or behaviour of FMLs in response to a bearing load configuration.

Pin and bolt bearing experiments were performed by Slagter [2] on both an Aramid Reinforced Aluminum Laminate (ARALL) and GLARE FMLs with an emphasis placed on the extraction of bearing strength values governed by a bearing failure mode only. While generating bearing strength data, it was observed that specimens with finger-tightened, lateral restraints exhibited a marked increase in strength. This boost in bearing strength did not change considerably with a proportional increase in the tightness of the lateral restraint and it was proposed that the additional boundary condition provided a restriction of delamination and buckling of the aluminum layers. Since the delamination buckling preceded joint collapse, it was also proposed that this phenomenon was ultimately responsible for the failure of the joint.

Van Rooijen *et al* [5] investigated numerous edge-distance-to-diameter ratios (e/D) and width-to-diameter ratios (W/D) while conducting finger-tightened bolt bearing experiments on a GLARE 2 FML. FE models were generated with good agreement to the empirical results; however, a

prediction of joint strength or behaviour using the concept of characteristic dimensions – although briefly mentioned – was dismissed and not examined any further.

In general, there exists a notable deficit in the literature regarding the strength and behaviour of GLARE in response to a bearing load configuration. As a consequence, the need for an experimentally validated prediction methodology is evident and the successful development of one would prove to be a valuable design tool. The focus of this manuscript is the proposal of a novel bearing strength prediction methodology incorporating aspects of both a theoretical and empirical nature.

2 Proposed Methodology

2.1 Prediction of Bearing Failure

Bearing failure in mechanically fastened, conventionally laminated composites has been successfully predicted using the characteristic length method developed by Chang et al. [6]. However, a direct application of this method to hybrid composites such as GLARE is not possible due to their two-phase through the thickness structure.

Krimbalis *et al* [7] investigated the bearing behaviour of GLARE FMLs employing layer by layer FE models of the laminates which were geometrically similar to experimental configurations for bearing strength testing as depicted in Fig. 1.

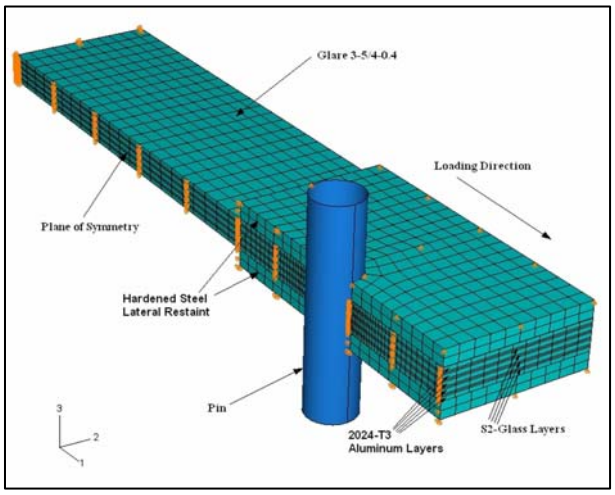

Fig. 1. Typical geometry of the FE models used in the modified CCD extraction and failure prediction.

In addition, an orthotropic plate buckling analysis of the glass prepreg layers was conducted to quantitatively assess the contribution to bearing strength provided by the glass fibre layers, which due to their brittle nature, are not prone to yielding.

It was shown, analytically, that as a consequence of the delaminated area – of which the concomitant is a lack of lateral support – the contribution of the fibre layers to bearing strength was negligible and therefore the bearing strength of a mechanically fastened hybrid material can be said to be governed by the behaviour of a single constituent: the aluminum. It was this result, among others, which prompted a new redefinition of the CCD. By defining the CCD as a parameter governed by the yield strength of the aluminum layers, the observed failure through delamination buckling phenomenon is ultimately incorporated.

Through subsequent post processing of the FE models, plots of compressive stress versus increasing distance from fastener hole can be created yielding a profile which describes the strain field directly adjacent to and moving away from the fastener hole. An example of one of these plots using the Von Mises criterion and exhibiting a characteristic, rapid monotonic decay is shown in Fig. 2. The three curves represent, in order of decreasing stress, the aluminum, longitudinal fibre and transverse fibre layers respectively.

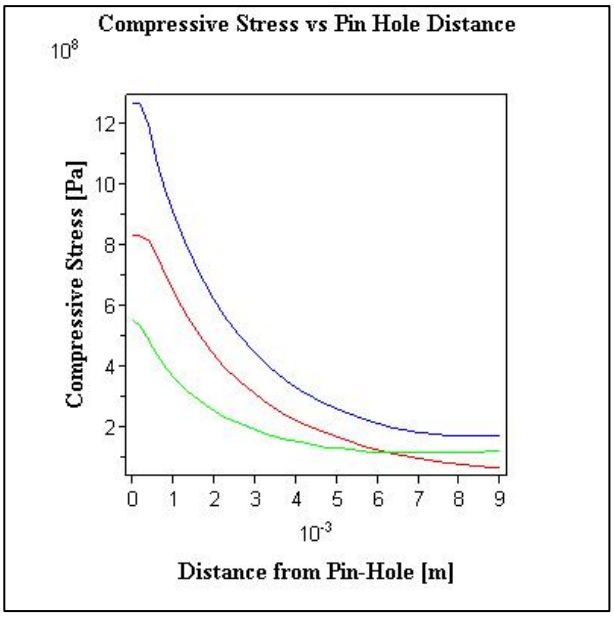

Fig. 2. Compressive stress vs. distance from fastener hole profile generated from FE results.

The new CCD was defined as the distance from the edge of the fastener hole in which the compressive stresses have fallen below that of the yield strength of the aluminum layers. Thus, the

value of the modified CCD is directly dependant upon the chosen criterion, be it the single axis S_{11} stress or the combined stresses given by Von Mises and Tresca. In order to calculate the CCD values from the aforementioned plots with sufficient accuracy, the precise value of the yield strength of the aluminum layers was specified to be $y = \sigma_{y,Al} =$ 345 MPa and the upper/lower bounds surrounding the distance from the fastener hole (the corresponding x-axis value) were interpolated using third order polynomials. A summary of the calculated CCD values for some of the GLARE variants analyzed can be found in Table 1.

Table 1: A summary of the calculated CCD values and their associated criteria.

GLARE Variant	Constituent	CCD for S_{11} [mm]	CCD for Von Mises [mm]	CCD for Tresca [mm]
GLARE 2-2/1-0.4	Al 2024-T3	2.814	3.800	4.350
	S_2 Glass L	2.328	2.431	2.514
GLARE 3-5/4-0.4	Al 2024-T3	3.157	3.886	4.362
	S_2 Glass L	2.571	2.659	2.721
	S_2 Glass LT	0.719	1.147	1.404
GLARE 4-3/2/-0.4	Al 2024-T3	3.032	3.866	4.372
	S_2 Glass L	2.471	2.555	2.619
	S_2 Glass LT	0.628	1.034	1.303

The near constancy of the calculated CCD values within each constituent of the compared GLARE variants suggests that the CCD, defined in this manner, may be a property of the material and independent of geometry or lay-up [7].

The CCD represents one of two global parameters employed in the calculation and subsequent plotting of the characteristic curve [6]. It is upon this curve that failure can be evaluated, rather that the edges of the fastener hole itself. The characteristic curve has seen much successful application in the prediction of failure in mechanically fastened composite joints and by virtue of the newly defined CCD, can now be extended to hybrid composites as well.

In addition and as a consequence of the new definition, a conservative estimation of the dimensions of the developed delaminated region adjacent to the fastener hole can be predicted. The boundaries of this rectangular shaped region are set by the extracted value of the CCD and within this predicted delaminated region, it is proposed that the aluminum layers have yielded, buckled and therefore failed, in a bearing mode [6].

2.2 Experimental Methodology

In order to validate the aforementioned predictions and study the range of predicted CCD values dependant upon the selected criterion, a novel experimental methodology was also required. Current standard test methods [8] for bearing strength measurement are designed for the calculation of bearing yield strength and bearing failure strength with little emphasis on capturing the strain field directly adjacent to the fastener hole.

Krimbalis et al. [9] developed a new experimental protocol extended from ASTM D953-02 [8] aimed at capturing the local deformation induced by a bearing load at discrete locations on the aluminum substrate of the laminate. Fig. 3. depicts a typical specimen with the inclusion of a bonded strain gauge, the location of which can be adjusted to correspond to the desired region of local strain measurement. Two distinct gauge locations were employed, both of which derive their position from the calculated CCD. The first position was set at 2.0 mm away from the fastener hole to be within the predicted yield range as calculated using the S_{11} criterion. The second position was at 4.0 mm away from the fastener hole to detect yield as predicted by the Von Mises and Tresca criteria.

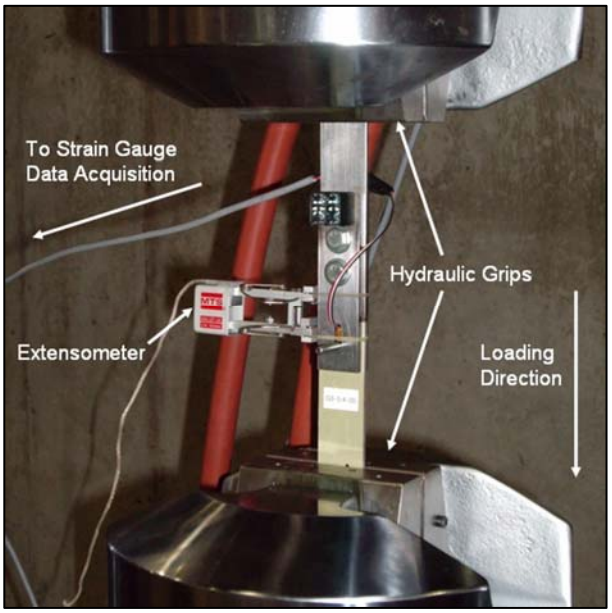

Fig.3. A typical test specimen with a bonded strain gauge at 2.0 mm away from the fastener hole.

The new protocol and added instrumentation enables the detection of yield in the aluminum layers

of the laminate, which is useful in determining bearing failure according to the aforementioned modified definition of CCD.

In addition to the local measurement of strain, a global measurement of deformation was performed as per the aforementioned standard using an extensometer [8]. Plots of applied stress versus extensometer displacement were generated, once again as per the standard and are shown in Fig.4. Failure in a bearing mode has been arbitrarily assigned as the force which corresponds to a 4% permanent hole deformation [8].

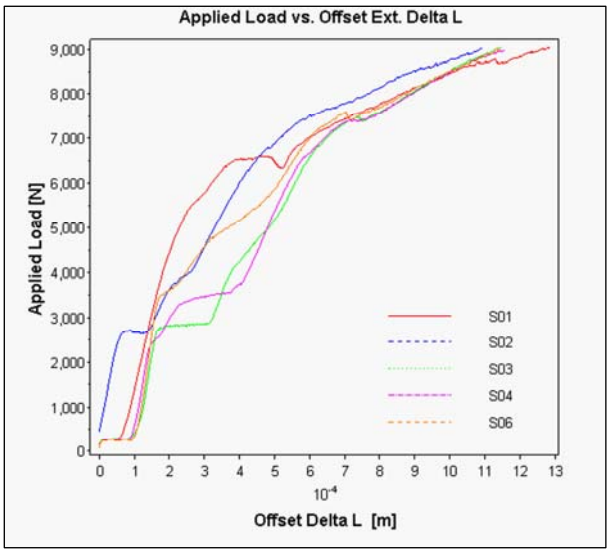

Fig.4. Bearing load vs. extensometer deformation curves for a typical GLARE variant. Note the plateaus and large statistical scatter.

It is clear that these plotted profiles are subject to numerous plateaus associated with pin seating and local deformation, as well as a very high statistical scatter. It is precisely these phenomena which suggest that viewing a pin bearing loading configuration from a global perspective is inadequate at capturing the events on the local scale which have been shown to govern the failure of the joint [7].

The modified protocol overcomes these problems with the use of local measurement. A pseudo-stress-strain curve for the characterization of the material's behaviour in response to this loading configuration can be plotted if the applied bearing stress is calculated via the following equation:

$$\sigma_b = \frac{P}{Dt} \qquad (1)$$

where P is the applied load, D is the hole diameter and t is the specimen's thickness.

When the calculated bearing stress is plotted against the measured strain as outputted from the attached strain gauge, the result is much more intuitive and not subject to any of the aforementioned phenomena present in the applied load versus extensometer displacement profiles. Fig. 5 shows some of the typical results of specimens prepared from a GLARE variant and subjected to a bearing load with the strain gauge located at 2.0 mm distal to the fastener hole. Note: these are the same specimens as plotted in Fig.4 but now subject to local strain measurement instead of a global one.

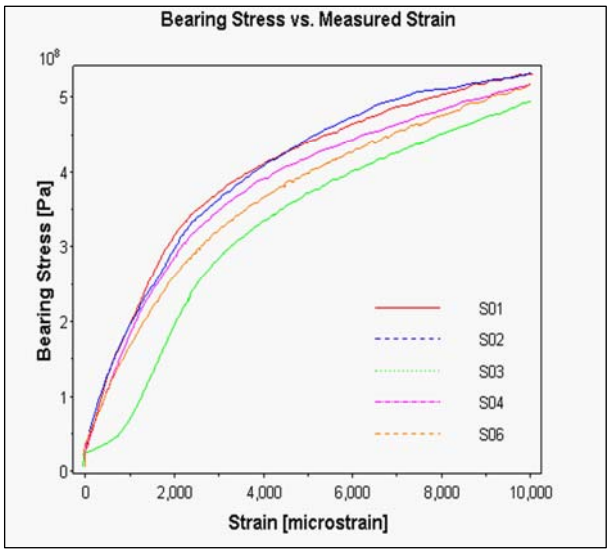

Fig. 5. Calculated bearing stress-strain curve for a typical GLARE variant. Note the absence of applied load plateaus and statistical scatter.

A close examination of Fig.5 reveals that as opposed to arbitrarily assigning an extensometer displacement as the point of yielding, the very geometry of each curve itself implies the onset of yield in a manner entirely analogous to a standard tensile test.

A complete characterization of the bearing stress versus measure strain curve is required to extract intuitive values for the onset of yielding. If viewed macroscopically, the above curves resemble two linear portions bridged by a non-linear portion in the middle strain regime. It would be remarkably convenient to apply a standard 0.2% offset technique on a curve of this nature and extract yield values without question; however, the loading configuration and two-phase-through-the-thickness-heterogeneity of GLARE does not lend itself to a direct application of this technique and the results would be suspect. For the sake of completeness though, such a technique was applied and it was

found that the point of yield far overshot the non-linear portion of the curve and entered the secondary, high strain, linear regime [9]. It is the intent of this study to incorporate said non-linear portion and thus the aforementioned characterization was completed employing the following piecewise function:

$$\sigma_b = \begin{cases} m_{el}\varepsilon + b_{el} & 0 \le \varepsilon \times 10^{-6} \le 2000 \\ -a + b_{nonlin}\ln(\varepsilon) & 2000 \le \varepsilon \times 10^{-6} \le 5000 \\ m_{pl}\varepsilon + b_{pl} & 5000 \le \varepsilon \times 10^{-6} \le 10000 \end{cases} \quad (2)$$

where the parameters m_{el}, b_{el}, a, b_{nonlin}, m_{pl} and b_{pl} are empirically derived values as a result of a minimization of the least squares error in response to the linear and logarithmic functions deployed to approximate the entire curve [9]. The effective domain on the non-linear portion of the curve and its accompanying logarithmic approximation changed slightly from specimen to specimen but never differed more than 10%.

Fig.6 depicts a direct comparison of a typically acquired data curve for a tested specimen and its subsequent characterization through the proposed piecewise function. The piecewise approximation clearly incorporates influence from the entire curve and offers an immediate improvement over a direct implementation of a 0.2% offset or an idealized bilinear approximation [9].

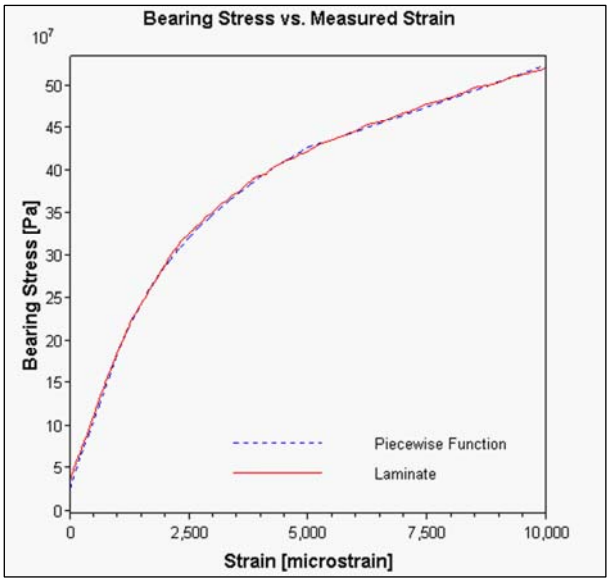

Fig. 6. Bearing stress vs. measured strain curve for a typical tested specimen. Note the accuracy of the piecewise approximation.

A more intuitive value for bearing yield strength can now be extracted from the piecewise approximation since influence from the entire curve is present in its calculation. A novel definition of bearing yield strength has been proposed and can be explained as follows: if the low and high strain linear portions of the curve are extended they will intersect at the so-called "knee-point" of the curve. A projection of this intersection through a bisection of the angle formed between the two linear portions onto the non-linear portion of the curve would be the newly defined value for bearing yield strength [9]. This value carries with it influence from the entire curve and does not from its definition rest heavily on arbitrarily defined values of offset. Fig.7 depicts a typical test specimen with the geometric interpretation of the newly defined bearing yield strength shown.

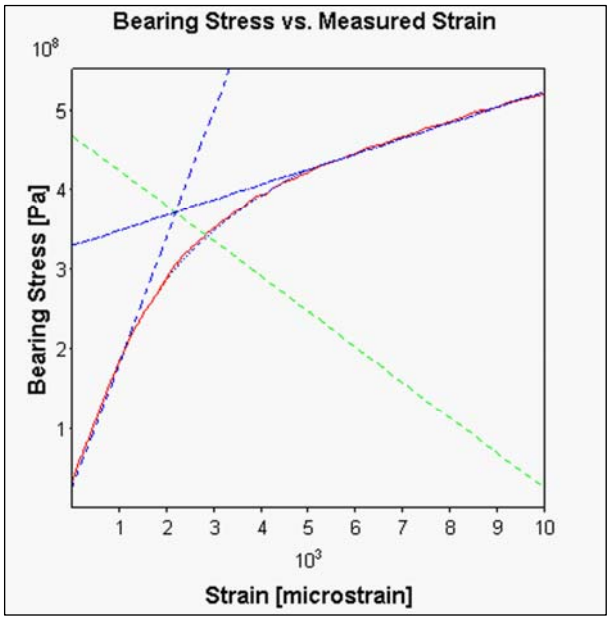

Fig.7. Bearing stress vs. measured strain curve for a typical GLARE specimen showing the applied bisection technique employed in the novel definition of bearing yield strength.

Preliminary results for specimens instrumented with strain gauges at 2.0 mm distal to the fastener hole reveal inter-variant bearing yield strength values between 340 MPa and 370 MPa with very small specimen to specimen statistical scatter [9]. Yielding, according to the proposed definition, has in fact occurred in the tested specimens within the distance prescribed by the S_{11} criterion's definition of the modified CCD. This failure is clearly shown in Fig. 8 with a distinct region of yielding and delamination buckling shown. Note that in Fig. 8 much of the deformation is out of plane but the failed region is unambiguous. This is quite encouraging, however, further work is required to repeat the yield strength extracting procedure for

gauges mounted 4 mm distally (with respect to the outputted distance defined by the Von Mises and Tresca criteria) and perhaps a third as yet undetermined location.

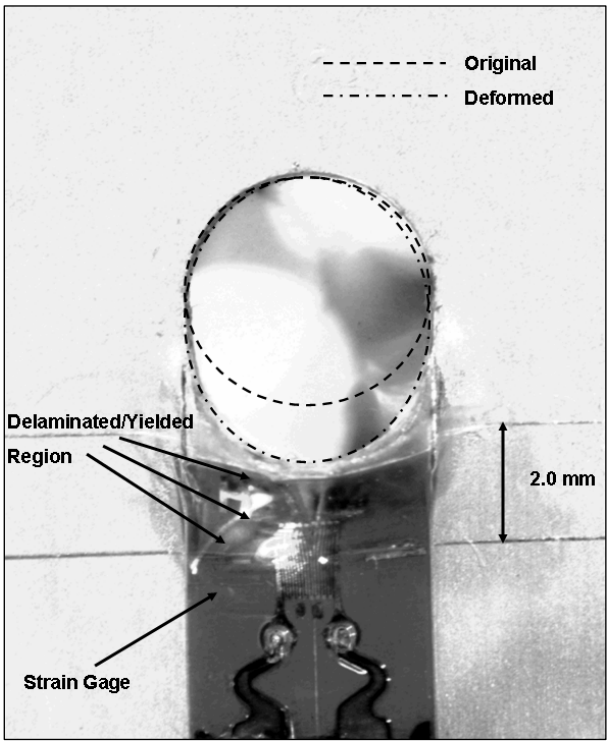

Fig. 8. Typical specimen showing failure in a bearing mode. Note the characteristic elongation of the fastener hole and the delaminated/yielded region with both in plane and out of plane deformation.

2.3 Proposed Validation

The modified CCD values extracted from the generated FE models predict a distance away from the fastener hole in which the compressive stresses have fallen below the yield strength of the aluminum layers. As a result, it is proposed that any material proximal to the fastener hole has delaminated and yielded, thus rendering the laminate failed in a bearing mode.

In order to validate these predictions a measurement of strain and detection of yield must be carried out at the discrete locations whose distance corresponds to the values of CCD generated according to the selected criterion. Employing the new experimental protocol enables the bonding of a strain gauge at these locations dictated by the calculated CCD and a direct measurement of local deformation and/or yielding can be made. As a result, the proposition of bearing strength being a parameter governed by the yield strength of the aluminum layers, coupled with delamination and buckling – as defined by the new CCD – can be experimentally verified.

In an ultimate sense, should yielding occur at the prescribed distances – and preliminary trials support this – the proposed damage prediction methodology for bearing failure in GLARE would be validated and can proceed as an effective tool for design. In a qualitative sense – better stated as the binary notion of whether or not the aluminum has yielded at or within the prescribed distance – the prediction, as outlined in the previous section, has been verified. The more quantitative comparison of outputted stresses and strains versus calculated/measured stresses and strains is currently underway.

The quantitative manner in which the output from the FE models can be directly compared to measured strain - via the bonded strain gauges - requires some additional consideration. Since the strain gauges themselves, although small in their dimension across the length of the foil, are in fact measuring strain over a finite area they, therefore, in principle cannot be explicitly defined as a point measurement of strain. In reality, the nodal values for field output variables as produced by the FE models need to be averaged over the length of the gauge. This can be accomplished by plotting nodal paths within the FE models corresponding to element lengths and thicknesses and the retrieved values for nodal output variables can then be averaged across the dimensions of the gauge.

An example of an exercise aimed at illustrating the above point is depicted in Fig. 9. Note the load applied in the exercise featured in Fig. 9 does not necessarily correspond to the failure load observed in the experimentation. It is merely a calibrated value employed to show how calculated stresses may vary from node to node within a single element of the model.

Each of the curves in Fig. 9 represents a nodal path moving distally from the fastener hole and whose corresponding origin initiates at one of the four corners of the hexahedral elements' square cross section. The mean value would then be an average path moving through the centre of the square cross section and thus through the middle of the hexahedral elements. The result of said averaging, shown in this highly magnified view, is a very small difference in S_{11} stress retrieved at each node within the square cross section. This differential is quantified by a coefficient of variation of only 1.98% along the entire length of the selected nodal paths. It can thus be argued that the variation

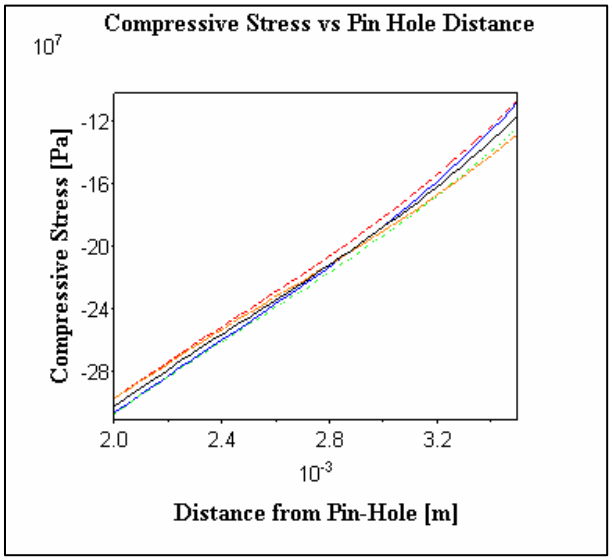

Fig. 9. Highly magnified view of a portion of the compressive stress vs. pin hole distance profiles showing the nodal variation of S_{11} outputted field variables from the corner nodes of a square cross section within a hexahedral element.

of stress through the thickness or across a single element face is quite small (a consequence of a highly refined mesh) and it is left to the discretion of the analyst to decide if the small improvement in the calculated result warrants the additional effort. For the sake of completeness the average value will be used in the validation.

With the nodal variation of field variables within an element's cross section evaluated, a direct comparison of the experimental and FE results should ensue.

It must be noted that a direct comparison of any of the outputted field variables for calculated stress is not possible with the calculated values taken from experimentation. The principal reason is that the bearing stress as calculated from the applied load in the experiment was found using Eq.1. As a result, any value calculated in this fashion ultimately includes the specimen thickness *t* and the hole diameter *D*. In comparison, none of the outputted field variables available directly from the model incorporate the hole diameter in their calculation.

In order to overcome this inherent incompatibility, two possible solutions are proposed herein that will be employed, among others, in the subsequent quantitative validation.

The first possibility is the request of nodal forces as a result of element stresses at each node of the elements to be outputted in tabular fashion. These values of force could then be directly implemented in a small routine which would calculate bearing stress according to Eq. 1 at nodal points moving away from the fastener hole. With a value of FE bearing stress calculated in the same manner as the bearing yield strength calculated from the experiment at a specific point distal to the fastener, a direct comparison can be made at the same distance in the model.

The second possibility is the creation of a user defined field output variable whose value can be calculated using Eq.1. In this sense, the amount of post processing is reduced to the simple act of plotting this user defined variable in a manner analogous to the S_{11}, Von Mises and Tresca field outputs plotted previously. However, there does not exist an intermediate set of output by which the analyst can check the results for possible errors.

Should either possibility be employed the result will still depend on a direct comparison to the experimentally calculated values of bearing stress at the specific point of measurement. As this is still a work in progress, at the time of this writing the chosen technique and quantitative evaluation are still currently under investigation.

3 Summary and Conclusions

The predictions and experimental methodologies aimed at validation discussed herein represent an approach to create a design tool based on both theoretical and empirical results. The notion of a laminate property's dependence on the response of a single constituent can be evaluated – with a precise yet intuitive convention – by the proposed experimental means.

In addition, the novel CCD and bearing yield strength definitions presented in the proposed methodology represent an extension of well defined parameters used with success in conventional materials that can now be applied with success to next generation materials which may display a hybrid or heterogeneous quality about them. The key to their successful implementation rests in an understanding of the hybrid material's constituents and applying both theoretical and empirical techniques to elucidate the identity and behaviour of the governing failure mechanism.

In conclusion, it is clear that the proposed failure through yielding and delamination buckling has been qualitatively verified in a binary "failed or not failed" sense within the predicted region dictated by the CCD. This result is quite encouraging though continued work is required and is currently underway to more precisely evaluate the validity of

the prediction and clearly identify its applicability as a useful design tool.

Acknowledgments

The authors wish to acknowledge the Natural Science and Engineering Research Council of Canada (NSERC) and the Ontario Graduate Scholarship (OGS) program of the Government of Ontario for their financial support, as well as Bombardier Aerospace Incorporated for their donation of GLARE materials.

References

[1] Roebroeks, G.H.J.J. (author), Vlot, A. and Gunnink, J.W. (eds.). "Glare Features". "*Fiber Metal Laminates an Introduction*". Kluwer Academic Publishers, 2001.

[2] Slagter, W.J. "On the Bearing Strength of Fiber Metal Laminates". *Journal of Composite Materials*, Vol. 26, No. 17, pp 2543-2566, 1992.

[3] Caprino, G., Squillace, A., Giorleo, L., Nele, L. and Rossi, L. "Pin and bolt bearing strength of fiberglass/aluminum laminates". *Composites: Part A*, Vol. 36, pp 1307-1315, 2005.

[4] Meola, C., Squillace, A., Giorleo, G. and Nele, L. "experimental characterization of an innovative glare® fiber reinforced metal laminate in pin bearing". *Journal of Composite Materials*, Vol. 37, No. 17, pp 1543-1552, 2003.

[5] Van Rooijen, R.G.J., Sinke, J., De Vries, T.J. and Van Der Zwaag, S. "The bearing strength of fiber metal laminates" *Journal of Composite Materials*, Vol. 40, No. 1, pp 5-19, 2006.

[6] Chang, F.K., Scott, R.A. and Springer, G.S. "Strength of mechanically fastened composite joints". *Journal of Composite Materials*, Vol. 16, November, pp 470-494, 1982.

[7] Krimbalis, P.P, Poon, C., Fawaz, Z. and Behdinan, K. "Prediction of bearing strength in fiber metal laminates". *Journal of Composite Materials*, In Press, 2006.

[8] "Standard test method for bearing strength of plastics." *Annual Book of ASTM Standards*, Item D953-02, 2002.

[9] Krimbalis, P.P., Poon, C., Fawaz, Z. and Behdinan, K. "Experimental characterization of the bearing strength of fiber metal laminates". *Journal of Composite Materials*, In-Press, 2007.